Heliyon 10 (2024) e29641

Contents lists available at ScienceDirect

Heliyon

journal homepage: www.cell.com/heliyon

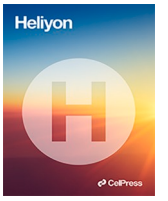

Research article

The green tide causative-species *Ulva prolifera* responding to exposure to oil and dispersant

Qing Liu, Ruifei Cui, Yuxin Du, Junjie Shen, Cuili Jin, Xiaojian Zhou *

Marine Science and Technology Institute, College of Environmental Science and Engineering, Yangzhou University, Yangzhou, 225127, China

ARTICLE INFO

Keywords:
Green tide
Oil spills
U. prolifera

ABSTRACT

In order to study the role of oil spills in the occurrence of green tide in the Yellow Sea, the physiological characteristics and photosynthetic activities of green tide causative-species *Ulva prolifera* was monitored under different conditions including two oil water-accommodated fractions (WAFs) of diesel oil and crude oil, dispersed water-accommodated fractions (DWAFs) and dispersant GM-2. The results showed that, the physiological parameters of *U. prolifera* including the growth, pigment, carbohydrate and protein contents decreased with the increased diesel oil WAF (WAF_{DO}) concentration, while crude oil WAF (WAF_{CO}) showed low concentration induction and high concentration inhibition effect. In addition, with the increase of WAFs concentration, two antioxidant activities were activated. However, compared with WAF_{DO} alone and WAF_{CO} alone, the mixture of oil and dispersant enhanced the toxicity on the above physiological characteristics of *U. prolifera*. On the other hand, the photosynthetic efficiency of *U. prolifera* showed a similar trend. Two WAFs showed significant concentration effects on the chlorophyll-*a* fluorescence transients and JIP-test. The addition of dispersant further blocked the electron flow beyond QA and from plastoquinone (PQ) to PSI acceptor side, damaged the active OEC centers at the PSII donor side, suppressed the pool size and the reduction rate of PSI acceptor side, and reduced the energy transfer efficiency between PSII functional units. These results implied that the crude oil spills may induce the formation of *U. prolifera* green tide, and the oil dispersant GM-2 used after the oil spills is unlikely to further stimulate the scale of bloom, while the diesel oil spills is always not conducive to the outbreak of green tide of *U. prolifera*.

1. Introduction

Offshore oil pollution mainly comes from offshore oil exploitation and ship leakage. From 2000 to 2019, approximately 1.5–10 million tons of petroleum hydrocarbons were spilled into seawater worldwide per year. In recent years, the oil spills accident in the Yellow Sea (YS) of China has aroused people's concern about petroleum hydrocarbon pollution. On November 22, 2013, an oil pipeline operated by Sinopec in Qingdao, resulted in spilled oil of about 2000 tons and the direct economic loss of about 751 million yuan [1,2]. On April 27, 2021, a ship collision occurred near the Qingdao port, spilling about 400 tons of oil into the YS [3]. Oil spill pollution not only caused a great economic damage, but also made a serious threat to the marine and coastal ecosystems.

The application of chemical dispersants is a commonly employed method for mitigating oil pollution following an oil spill incident. An oil dispersant is a blend of surfactants and solvents that serves to reduce the surface tension at the interface between the oil and

* Corresponding author.
E-mail address: zhouxiaojian@yzu.edu.cn (X. Zhou).

https://doi.org/10.1016/j.heliyon.2024.e29641
Received 22 March 2024; Received in revised form 8 April 2024; Accepted 11 April 2024
Available online 16 April 2024

water. This process aids in breaking down the oil into smaller droplets, allowing it to disperse and mix within the water column under the influence of wind and sea waves. By removing the oil from the water surface, the level of contamination along the coastline can be reduced. Dispersant has been routinely utilized worldwide, including during significant oil spill events such as the Gulf of Mexico disaster and the 2021 Qingdao oil spill. However, it is important to note that while the use of oil dispersants can be beneficial, there is also the potential for them to introduce secondary pollution to marine ecosystems [4]. Both petroleum hydrocarbons and dispersants can have adverse effects, highlighting the need for a careful assessment of the comparative toxicity of petroleum derivatives on marine environments resulting from oil spills.

Over the past few decades, there has been a notable increase in both the frequency and scale of harmful algal blooms (HABs) in coastal regions [5]. Recent studies have indicated a strong connection between the rising occurrence and severity of HABs and coastal oil pollution events [6]. The frequency of HABs has been found to be positively correlated with the number of oil spills and the volume of oil released. It has been observed that a higher proportion of smaller oil spills (<7 tons) are more likely to exacerbate the occurrence of HABs [7]. Large-scale algal blooms often follow an oil spill, sometimes occurring multiple times within weeks or months following the incident [8–10]. For instance, after the massive Deepwater Horizon oil spill in the United States in April 2010, satellite images (MODIS) revealed algal blooms approximately 20 days post-spill [8,9]. Furthermore, following a three-month-long oil spill incident in Penglai, Bohai Sea in June 2011, three successive phytoplankton blooms were observed in the surrounding waters [9]. These occurrences can be attributed to several factors: the application of dispersants, weathering processes, and biodegradation. These factors collectively lead to a reduction in the concentration of petroleum hydrocarbons and the size of oil droplets in seawater, with lower concentrations of hydrocarbons potentially stimulating algae growth. Additionally, oil spills and dispersants can disrupt predator-prey interactions within planktonic food webs and indirectly promote the initiation of HABs.

YS has experienced harmful algal blooms (HABs) over the past few decades. Recent studies have documented 165 red tide events between 1972 and 2017, along with 17 consecutive years of green tide occurrences from 2007 to 2023 in the YS region of China [11,12]. *Ulva prolifera*, a common green macroalgae found globally, is identified as the primary causative species responsible for the green tides in the YS. Due to its ease of propagation and strong adaptability to coastal environments, the substantial accumulation of *U. prolifera* biomass leads to the formation of large-scale green tides [13]. However, the exact role of oil spills in triggering *U. prolifera* green tides remains unclear. Some studies have suggested that the presence of petroleum hydrocarbons can reduce the growth rate of *Ulva* sp. Additionally, the pigment and glycolipid content within the cells may also undergo alterations [14]. Furthermore, various types of oils and components of dispersants can impact the occurrence of HABs. Oil spills in the YS typically involve crude oil from offshore drilling activities and diesel oil from ships. Dispersants like GM-2 and Corexit 9500 are commonly employed to mitigate oil spills in the region. Despite the use of dispersants, there is limited published data available on the impact of oil spills and GM-2 dispersants on the green tide species *U. prolifera*. Therefore, conducting a comparative assessment of the toxic effects of petroleum-derived substances, including oils, dispersants, and their combinations, on *U. prolifera* could shed light on the mechanisms underlying the outbreak of green tides in the YS.

In order to answer the above question, the toxicity of two kinds of oils water-accommodated fractions (WAFs), chemical dispersant GM-2 (D) and their dispersed water-accommodated fractions (DWAFs) to *U. prolifera* was tested. Through analyzing the changes of physiological characteristics and photosynthetic activities under petroleum contamination stress, this work aims to reveal the link between oil spills events and *U. prolifera* green tide in the YS.

2. Materials and methods

2.1. Macroalgae culture

Macroalgae *U. prolifera* were collected from the coast of Qingdao. Thalli were washed several times with sterile seawater, gently cleaned with soft brushes and checked under a microscope to ensure that they were free of epiphytes. The treated *U. prolifera* thalli were controlled in a laboratory environment for several days prior to experiments. *U. prolifera* were cultured using f/2 medium, which was constituted of 75 g/L $NaNO_3$, 5 g/L $NaH_2PO_4{\cdot}H_2O$, 0.5 mL/L vitamin solution and 1 mL/L trace element solution. The detail composition was described by Guillard [15]. The thalli were maintained at 24 ± 2 °C, under an irradiance of 4000 lx, with a light: dark cycle of 12 h:12 h.

2.2. Test solution preparation

Diesel oil, crude oil and oil dispersant GM-2 were used in tests. Diesel oil and crude oil was produced from China Sinopec Co. Ltd. Dispersant GM-2 was obtained from Qingdao Guangming Environmental Technology Co. Ltd. The preparations of diesel oil WAF (WAF_{DO}) and crude oil WAF (WAF_{CO}) were in accordance with Singer et al. [16], Wilson and Ralph [17]. A vortex was created prior to the addition of oils to decrease the amount of oils adhered to the inside of the flask. Oils were added close to the water surface using a glass pipette. To prepare the WAFs, mixed the sterile seawater and oils in a flask (1:10 v/v), and stirred with a magnetic stirrer for 24 h at 150 rpm. Then the lower oil-seawater mixture was collected into a brown bottle by siphoning and stored at 4 °C. The preparation method of DWAFs is the same as above, and the ratio of dispersant to oil was 1:10 (v/v). The concentrations of WAFs and DWAFs were measured by UV spectrophotometer (UNICO, UV 2102-C, China).

2.3. Experimental design

All experiments were carried out in flasks containing f/2 medium, with the initial culture concentration of *U. prolifera* set at 1 g/L. The experimental design for the microcosm studies is presented in Fig. 1. 1) a control group with sterilized seawater only, 2) three groups exposed to WAF of diesel oil alone, 3) three groups exposed to WAF of crude oil alone, 4) a dispersant-only group, 5) a group exposed to DWAF of diesel oil, and 6) a group exposed to DWAF of crude oil. The WAF concentrations of diesel oil and crude oil in the experimental groups were set at 3 mg/L, 6 mg/L, and 12 mg/L each. The DWAF concentrations of diesel oil and crude oil in the experimental groups were both 3 mg/L. Each treatment consists of 12 flasks, and 3 flasks were taken out to test the following parameters at each time point (24 h, 72 h, 120 h, and 168 h). These exposure experiments were carried out for a duration of 7 days.

2.3.1. Specific growth rate (SGR)

The SGR was calculated using the following formula based on the macroalgae weight:

$$SGR = [ln(W_t / W_0) / t] \times 100\% \quad (1)$$

(where W_t, the wet weight of *Ulva* at the end of the experiment; W_0, the wet weight of *Ulva* at the begin of the experiment; and t, experimental time).

2.3.2. Chlorophyll-a and carotenoid contents

The content of chlorophyll-*a* (chl-*a*) and carotenoid (car) in the sample was determined according to the method by Porra [18] and Parsons et al. [19]. In detail, 0.1 g *Ulva* sample was added to 10 mL methyl alcoho and kept overnight at 4 °C in dark. Cell contents were lysed on the ice by an ultrasonic cell disruptor for 10 min (each 5s working with a 3s interval, 700W). Cell debris was removed by centrifugation (2500 r/min, 10 min, 4 °C), and the supernatant was retained to measure the optical density at 480, 510, 652 and 665 nm wavelength. The pigment concentration was calculated according to the formula:

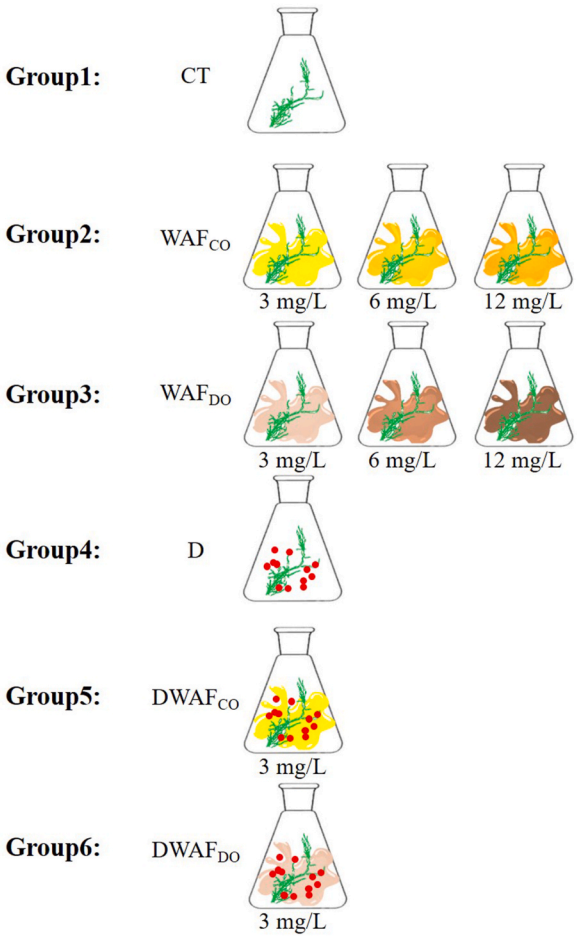

Fig. 1. The schematic diagram of the experimental design.

$$Chl-a = (16.29 \times OD_{665} - 8.54 \times OD_{652}) \times V / W \quad (2)$$

$$Car = 7.6 \times (OD_{480} - 1.49 \times OD_{510}) \times V / W \quad (3)$$

(where V, the methanol content; W, the weight of *Ulva*).

2.3.3. Cellular carbohydrate and protein contents

The carbohydrate and protein contents were measured using the phenol sulphuric acid method and Kaumas blue method, taking D-glucose and bovine serum albumin as standards, respectively [20,21]. In detail, 0.1 g *Ulva* sample were added 5 mL phosphate buffer (50 mmol/L, pH7.0) and grinded in the homogenizer. The homogenates were lysed on ice by an ultrasonic cell disruptor for 10 min until there was were no particles. After centrifugation at 3500 r/min, 4 °C for 10 min, the supernatant was used for carbohydrate or protein content measurement.

2.3.4. Superoxide dismutase and catalase activities

The activity of superoxide dismutase (SOD) was measured by the reduction of nitrite. The activity of catalase (CAT) was measured by the amount of product combining by H_2O_2 and ammonium molybdate. Two antioxidant enzymes were determined as described by Ramadass et al. [22]. Microplate reader was used to measure the spectrophotometric value of the reagent. All the reagents used were from commercial kit (A001–1–1 for SOD, A007–1–1 for CAT, Nanjing Jiancheng Bioengineering Institute, China).

2.3.5. Chlorophyll-a fluorescence parameters

Chl-*a* fluorescence was performed using Imaging PAM (AquaPen AP110, Photon Systems Instruments, Czechia). After 168 h of treatment, at least three *U. prolifera* samples in each treatments were measured after 15 min of dark adaptation. Analysis of OJIP transient parameters were conducted according to Stirbet [23], all parameters and their description are summarised in Table 1.

2.4. Statistical analysis

All the test parameters were calculated as the means ± standard deviations, and $P < 0.05$ indicated significant statistical differences between different treatment. The two-way ANOVA was used to analyse the effects of petroleum derivatives, time and the interactions

Table 1
OJIP test parameters and expressions.

Parameter	Formula	Description
F_O, F_J, F_I, F_K		Fluorescence intensity at 50 μs, 2 ms, 30 ms, 300 μs
F_M (F_P)		Maximal fluorescence intensity (P step); the peak of OJIP curve
F_V	F_M-F_O	Maximal variable fluorescence
V_J	(F_J-F_O)/(F_M-F_O)	Relative variable fluorescence at 2 ms
V_I	(F_I-F_O)/(F_M-F_O)	Relative variable fluorescence at 30 ms
V_t	(F_t-F_O)/(F_M-F_O)	Relative variable fluorescence at time t
W_{OJ}	(F_t-F_O)/(F_J-F_O)	Ratio of variable fluorescence (F_t –F_O) to the amplitude (F_J–F_O), used to show K-band
W_{OI}	(F_t-F_O)/(F_I-F_O)	Ratio of variable fluorescence (Ft –F_O) to the amplitude (F_I–F_O), used to show J-step
M_O	4 × (F_K-F_O)/(F_M-F_O)	Approximate initial slope of the fluorescence transient normalized on the maximal variable fluorescence Fv
OEC centers	$[1-(V_K/V_J)]_{treatment}/[1-(V_K/V_J)]_{control}$	The active fraction of oxygen evolving complexes centers
φ_{PO}	(F_M-F_O)/F_M = 1- (F_O/F_M) = F_V/F_M	Maximal quantum yield of PSII primary photochemistry
ψ_O	1-V_J	Probability that an electron moves further than Q_A
φ_{EO}	[1- (F_O/F_M)] × (1-V_J)	Quantum yield for electron transport
φ_{DO}	1 – φ_{PO}=(F_O/F_M)	Quantum yield of energy dissipation
δ_{RO}	(1-V_I)/(1-V_J)	Efficiency/probability with which an electron from the intersystem electron carriers is transferred to reduce end electron acceptors at the PSI acceptor side (RE)
ABS/RC	(TRo/RC)/(TRo/ABS)	Average absorbed photon flux per active RC
TRo/RC	4 × (F_K-F_O)/(F_J-F_O)	Maximum trapped electron flux per active RC
ETo/RC	(TRo/RC)(1–V_J)	Electron transport flux per active RC
DIo/RC	ABS/RC–TRo/RC	Energy flux dissipated as heat in active RC
ABS/CS_m	F_M	Average absorbed photon flux per cross section (at t = m)
TRo/CS_m	φ_{PO} × (ABS/CSm)	Maximum trapped electron flux per cross section (at t = m)
ETo/CS_m	φ_{EO} × (ABS/CSm)	Electron transport flux per cross section (at t = m)
DIo/CS_m	(ABS/CSm)-(TRo/CSm)	Energy flux dissipated as heat in cross section (at t = m)
RC/CS_m	φ_{PO} × (V_J/Mo) × (ABS/CS_m)	Number of the active reaction center per cross section (at t = m)
PI_{ABS}	(RC/ABS) × [φ_{PO}/(1-φ_{PO})] × [ψ_O/(1-ψ_O)]	Performance index (based on absorption)
PI_{CS}	(RC/CS_m) × [φpo/(1-φpo)] × [ψo/(1-ψo)]	Performance index (based on cross section)
PI_{TOTAL}	PI_{ABS} × [δ_{RO}/(1- δ_{RO})]	Performance index (potential) for energy conservation from photons absorbed by PSII antenna until the reduction of PSI acceptors

of them. Then, the effects of petroleum derivative at each fixed time and the effects of time at each fixed petroleum derivative were calculated by one-way ANOVA. The Pearson coefficient (r) was used to reveal the correlation between test parameters of *U. prolifera*.

3. Results

3.1. Effects of petroleum derivatives on the growth of U. prolifera

The SGR of *U. prolifera* under different stresses and exposure durations was shown in Fig. 2. In terms of dose effect, the SGR decreased with the increase of WAF_{DO} concentration, but low concentration induction and high concentration inhibition appeared under WAF_{CO} treatment. The impacts of WAF_{DO} were notably higher than those of WAF_{CO} at the same concentration ($P < 0.05$). Meantime, the inhibitory effects were significantly greater in the DWAF-treated groups than in the groups exposed to oil WAFs alone, for both diesel oil and crude oil ($P < 0.05$). Regarding the time effect, the SGR of *U. prolifera* exhibited a significant decrease followed by an increase in the 6–12 mg/L WAF_{DO}, 12 mg/L WAF_{CO}, and the three oil-dispersant combined groups. Conversely, the SGR showed an initial increase followed by a decrease in the groups treated with 3 mg/L WAFs.

3.2. Effects of petroleum derivatives on the pigment contents of U. prolifera

Fig. 3 showed the pigment changes of *U. prolifera* under different stresses and exposure durations. It can be seen that in terms of dose effect, when exposure to WAF_{DO}, D and DWAFs groups, the chl-*a* and car content of *U. prolifera* were all inhibited. Under the WAF_{CO}-exposure condition, *U. prolifera* appeared low concentration induction and high concentration inhibition effect. Meantime, the pigment contents decreased with the increase of WAFs concentration, the inhibitory effects of diesel oil were significantly higher than crude oil at the same concentration ($P < 0.05$). In addition, the decrease of pigment contents in DWAFs treatments were higher than WAFs treatments at the same concentration and dispersant alone treatments. In terms of time effect, except 6 mg/L WAF_{CO} showed an increasing trend and $DWAF_{DO}$ showed a decreasing trend on pigment contents with time, other treatment groups showed no significant change over time.

3.3. Effects of petroleum derivatives on the carbohydrate and protein contents of U. prolifera

The carbohydrate and protein contents of *U. prolifera* under different stresses and exposure durations was presented in Fig. 4. Regarding the dose effect, the carbohydrate and protein content of *U. prolifera* generally decreased with the increase of WAF_{DO} concentration, while its content appeared low concentration induction and high concentration inhibition effect under WAF_{CO} treatment. In addition, the $DWAF_{DO}$ treatments had no significant difference from WAF_{DO} treatment at the same concentration and D alone treatment ($P > 0.05$), which is the same as the difference between $DWAF_{DO}$ and $DWAF_{CO}$. While the decrease of carbohydrate and protein contents in $DWAF_{CO}$ treatments were higher than WAF_{CO} treatment at the same concentration. In terms of time effect, only 6–12 mg/L WAF_{CO} showed a notably increasing trend on carbohydrate and protein contents with time, no significant changes were observed in other treatment groups with time.

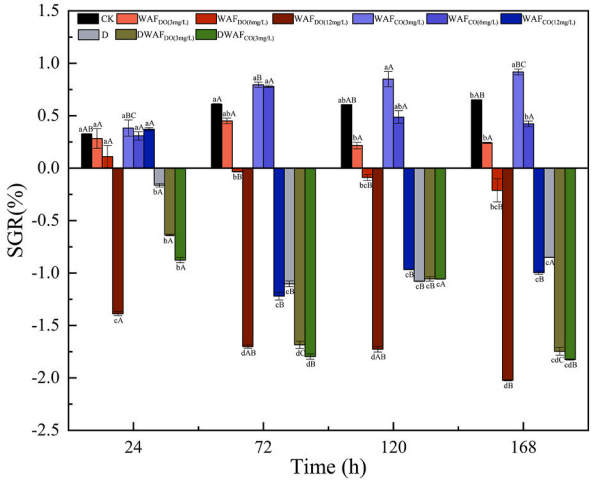

Fig. 2. The specific growth rate (SGR) of *Ulva prolifera* under different petroleum derivative stresses and exposure durations. Different capital letters and lowercase letters indicate significant differences between different time at the same stress and different stress at the same time, respectively ($P < 0.05$).

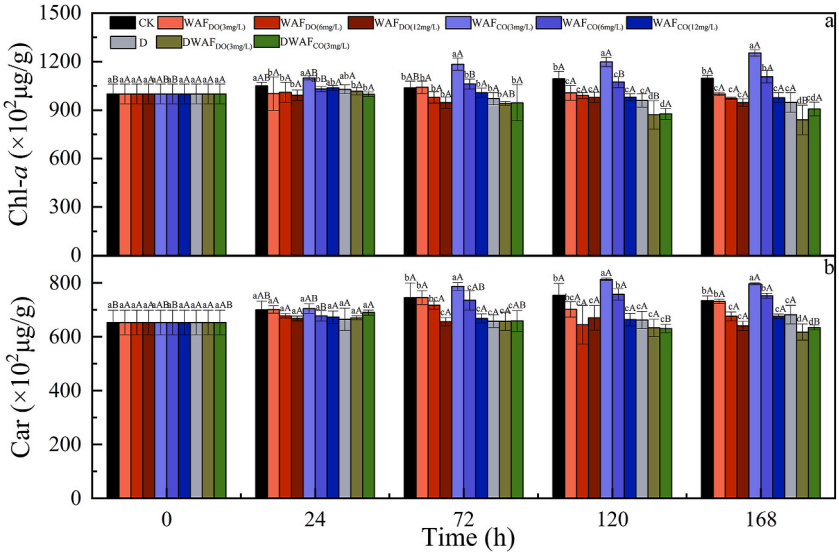

Fig. 3. The pigment content of *Ulva prolifera* under different petroleum derivative stresses and exposure durations (a. chl-*a*; b. car). Different capital letters and lowercase letters indicate significant differences between different time at the same stress and different stress at the same time, respectively ($P < 0.05$).

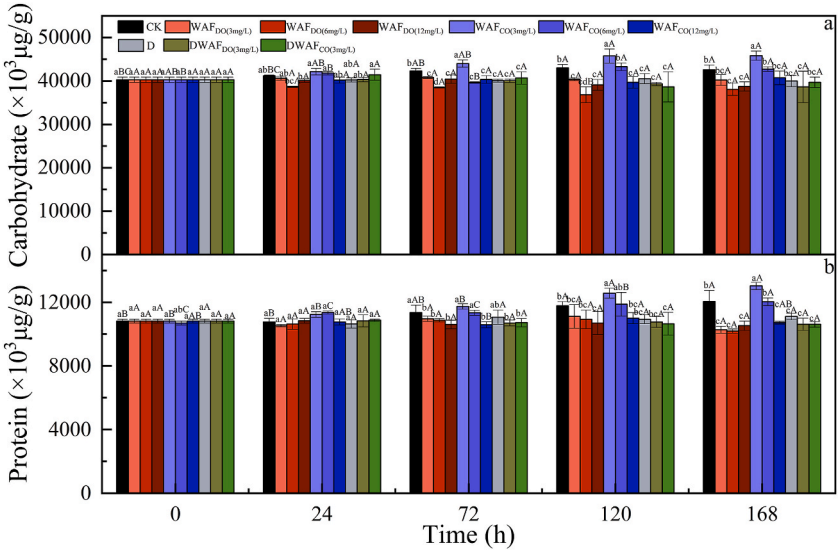

Fig. 4. The carbohydrate and protein contents of *Ulva prolifera* under different petroleum derivative stresses and exposure durations (a. carbohydrate; b. protein). Different capital letters and lowercase letters indicate significant differences between different time at the same stress and different stress at the same time, respectively ($P < 0.05$).

3.4. Effects of petroleum derivatives on the antioxidase activities of U. prolifera

Fig. 5 showed the antioxidant system changes of *U. prolifera* under different stresses and exposure durations. Regarding the dose effect, the SOD and CAT activity of *U. prolifera* had the significantly positive correlation with the concentration of WAFs at each period except WAF_{CO} at 72–120 h on SOD. In addition, the activities of two antioxidase were also increased at oil-dispersant addition groups. The promotion effect of $DWAF_{DO}$ was greater than WAF_{DO} and $DWAF_{CO}$. For CAT activity, dispersant-only group had the highest promotion effect than other groups. In terms of time effect, for SOD activity, except 3–6 mg/L WAF_{CO} showed an decreasing trend, 6–12 mg/L WAF_{DO} and $DWAF_{DO}$ showed a increasing trend with time, the trends for other treatment groups were not significant over time. For CAT activity, except 6 mg/L WAF_{DO}, 6–12 mg/L WAF_{CO}, D and $DWAF_{DO}$ showed an increasing trend with time, other treatment groups had no notably changes over time.

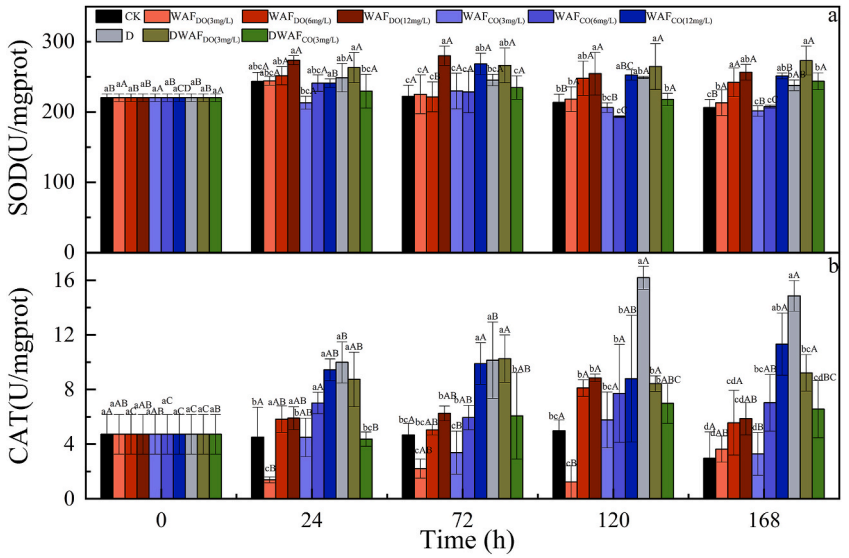

Fig. 5. The antioxidase activtities of *Ulva prolifera* under different petroleum derivative stresses and exposure durations (a. SOD; b. CAT). Different capital letters and lowercase letters indicate significant differences between different time at the same stress and different stress at the same time, respectively ($P < 0.05$).

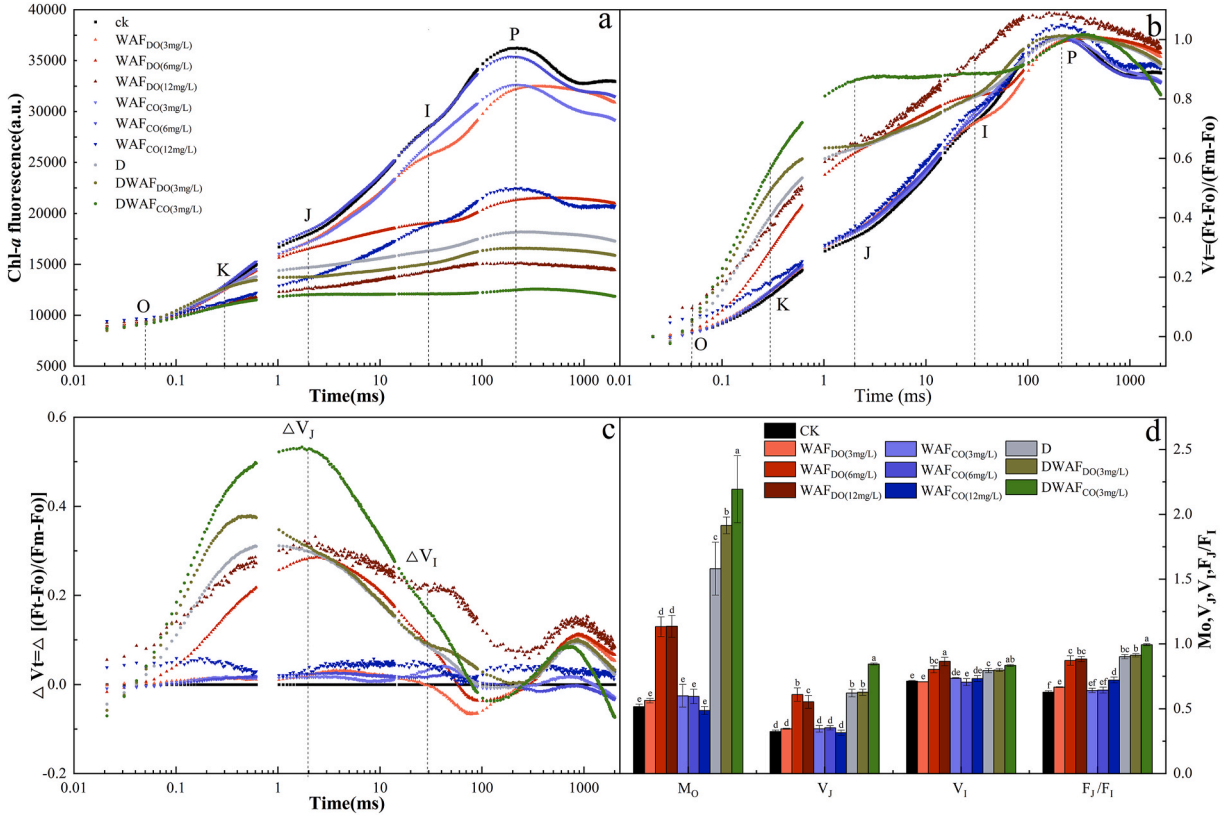

Fig. 6. Effects of petroleum derivatives on raw fluorescence rise kinetics OJIP curves and the relative variable fluorescence of *Ulva prolifera*. (a. chl-*a* fluorescence rise kinetics; b. chl-*a* fluorescence rise kinetics normalized by F_O and F_M as $V_t = (F_t - F_O)/(F_M - F_O)$; c. $\Delta V_t = V_t$ (treatment) - V_t (control); d. the value of M_O, V_J, V_I and F_J/F_I).

3.5. Effects of petroleum derivatives on the chl-a fluorescence of U. prolifera

3.5.1. Fluorescence rise kinetics OJIP curves

The analysis of fluorescence rise kinetics OJIP curves of *U. prolifera* in Fig. 6a showed that, compared with control group, the fluorescence intensity of J, I and P points decreased, indicating that the oxidation degree of electron transport chain decreased after dark adaptation. In detail, fluorescence emission was significantly decreased with the elevated WAF_S concentrations, addition of dispersant led to fluorescence intensity decreased rapidly. The OJIP rising kinetics in 6–12 mg/L WAF_{DO}, DWAFs and D groups were not obvious, which indicated that these treatments caused photo-oxidation damage of *U. prolifera*. The relatively variable fluorescence Vt (Fig. 6b) and ΔVt (Fig. 6c) to show the detailed characteristics of chl-*a* fluorescence rise kinetics. Compared to control, all the treatments especially 6–12 mg/L WAF_{DO}, D and DWAFs showed chl-*a* fluorescence drastically increased at J-step and I-step. Rapid rise of I-step indicate limited electron transfer from plastoquinone (PQ) to the PSI acceptor side. Sharp rise of J-step contributed to the large accumulation of QA^- in PSII reaction center (RCs) for the blockage of electron flow beyond QA. An increase in QA^- concentration will lead to the inactivation of PSII RCs. Mo is the approximate initial slope of F_V, representing the net rate of the RCs closure. It can be seen that the Mo values of D, DWAFs and 6–12 mg/L WAF_{DO} were significant higher than control ($P < 0.05$, Fig. 6d). To further evaluate the initial action site, three JIP test parameters, V_J (relative variable fluorescence at the J-step), V_I (relative variable fluorescence at the I-step) and F_J/F_I, were compared in Fig. 6d. At all treatment groups, only the V_J, V_I and F_J/F_I values of 6–12 mg/L WAF_{DO}, D and DWAFs were significantly increased, indicating the electron flow outside QA, from PQ to PSI acceptor side were all blocked under these stresses.

To detect the events reflected in the OK, OJ, OI and IP phase, other normalizations and corresponding subtractions (difference kinetics) were also performed in Fig. 7. Chl-*a* fluorescence rise kinetics curves were double normalized by O-step (50 μs) and K-step (300 μs) to show L-band, and W_{OK} (top) and ΔW_{OK} (bottom) in the linear time scale from 0 to 300 μs were presented in Fig. 7a. The L-band is considered as an indicator of the energetic connectivity or grouping of the PSII units. It clearly showed that the 12 mg/L WAF_{DO} and WAF_{CO}, D and DWAFs treatment groups significant increased L-band. Meanwhile, the W_L, ΔW_L and F_L/F_J values of above treated groups increased significantly compared with the control (Fig. 7b). This suggests that stress reduce the energy transfer efficiency

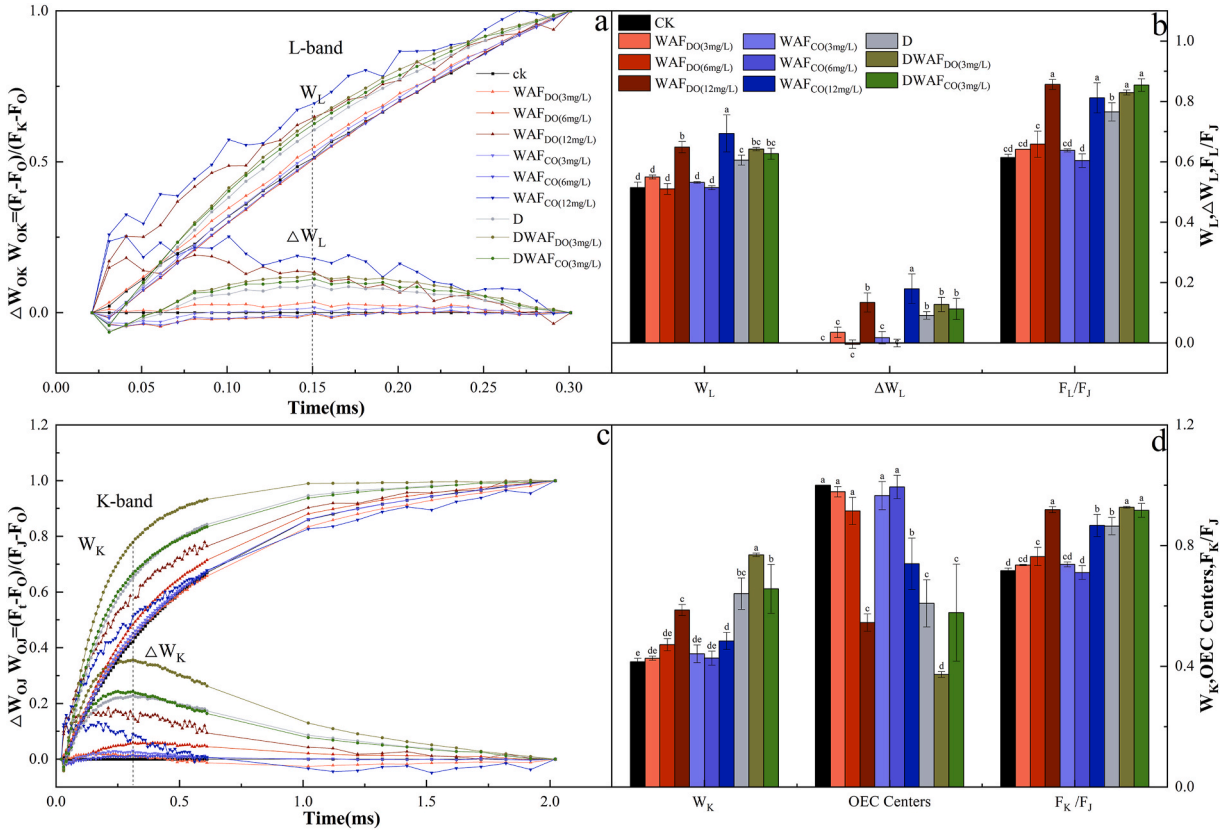

Fig. 7. Different normalizations of the fluorescence rise kinetics OJIP curves of petroleum derivatives treated *Ulva prolifera*. (a. the fluorescence rise kinetics normalized by F_O and F_K as $W_{OK} = (F_t - F_O)/(F_K - F_O)$ (top), and the difference kinetics $\Delta W_{OK} = W_{OK}$ (treatment) - W_{OK} (control) (bottom) in a linear time scale from 0 to 300 μs; b. the value of W_L, ΔW_L and F_L/F_J; c. the fluorescence rise kinetics normalized by F_O and F_J as $W_{OJ} = (F_t - F_O)/(F_J - F_O)$ (top), and the difference kinetics $\Delta W_{OJ} = W_{OJ}$ (treatment) - W_{OJ} (control) (bottom) in a linear time scale from 0 to 2 ms; d. the value of W_K, OEC centers and F_K/F_J).

between PSII functional units, decrease the electron transfer energy, and increase the light energy dissipation. In addition, to investigate the effects of variable treatments on the K-step, chl-*a* fluorescence rise kinetics were normalized by O-step (50 μs) and J-step (2 ms), and W_{OJ} and ΔW_{OJ} in the linear time scale from 0 to 2 ms were presented in Fig. 7c. ΔW_{OJ} curves showed that different treatments induced the appearance of the K-band, especially DWAFs, D and 12 mg/L WAFs groups. The increase of the K-step indicates the inactivation of OEC centers at the PSII donor side (Fig. 7d).It was found that above treatment groups significant increased in W_K and F_K/F_J ($P < 0.05$), decreased in OEC centers ($P < 0.05$) (Fig. 7cd), which confirmed that these stress damage the fraction of active OEC centers.

The fluorescence kinetics curves between the O-step and I-step (30 ms) were normalized as W_{OI} and ΔW_{OI} (Fig. 8a), as well as $W_{OI} \geq 1$ plotted in the linear 30–270 ms time range to show the IP phase (Fig. 8b). The smaller amplitude of the W_{OI} curve, the stronger the inhibitory effect on the cell size at PSI receptor side. Obviously, all treatment groups reduced the amplitude of W_{OI} curves to some extent, especially for $DWAF_{CO}$, 6–12 mg/L WAF_{DO}, D and $DWAF_{DO}$ groups. Another fluorescence rise kinetics normalization W_{IP} (normalized by I-step and P-step) was also shown in Fig. 8c. It can be seen that the half rise-time of the rise curves $W_{IP} = 0.5$ were greater in all treatment groups than in the control groups. This suggests that WAFs and DWAFs decrease reduction rates of PSI end electron acceptors pool. In Fig. 8d, δRo is a JIP test parameter that represents the probability of electron transport from the reduced intersystem electron acceptor to the final electron acceptor of PSI. It was found that δRo was significantly increased at D and DWAFs treatments. This means that the addition of dispersant would stimulate PSI activity partially.

3.5.2. *The JIP-test analysis*

In order to further assess the stress on the photosynthesis, several JIP test parameters were provided in Fig. 9. Firstly, the quantum yields represent the efficiencies of electron transport, including φ_{Po} (the maximal quantum yield of PSII primary photochemistry), Ψ_o (the probability that an electron moves further than QA), φ_{Eo} (the quantum yield for electron transport) and φ_{Do} (the quantum yield of energy dissipation). With increased WAF_s concentration, φ_{Po}, Ψ_o and φ_{Eo} declined significantly, while φ_{Do} showed the opposite trend (Fig. 9a). In addition, the values of φ_{Po}, Ψ_o and φ_{Eo} in the $DWAF_s$ groups were significantly lower than WAF_s groups at the same concentration, while φ_{Do} was significantly higher. The inhibition or promotion effects of $DWAF_{CO}$ was greater than $DWAF_{DO}$ and D treatment. Secondly, in terms of the specific energy flux per reaction centers (RC), the absorbed (ABS/RC), trapped (TRo/RC),

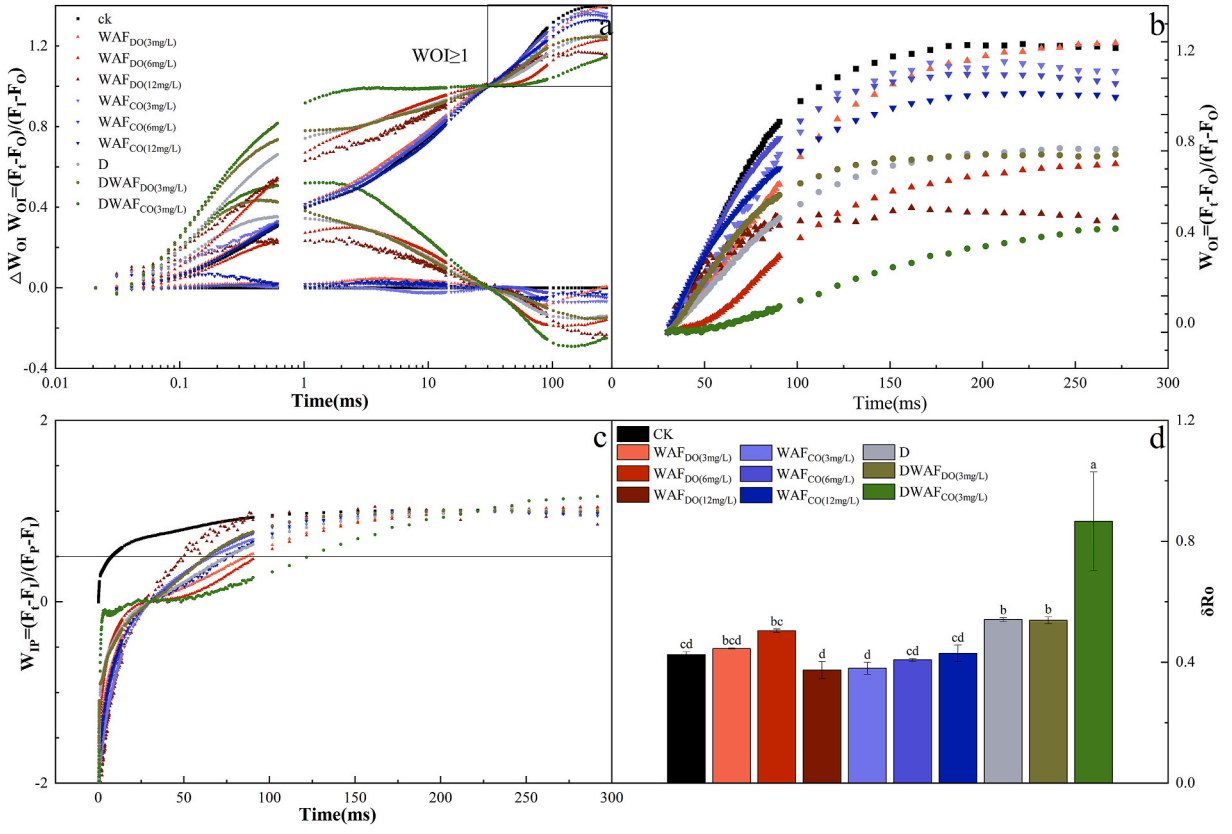

Fig. 8. Different normalizations of the fluorescence rise kinetics curves of petroleum derivatives treated *Ulva prolifera*. (a. the fluorescence rise kinetics curves normalized by F_O and F_I as $W_{OI} = (F_t - F_O)/(F_I - F_O)$ (top) and the difference kinetics $\Delta W_{OI} = W_{OI}$ (treatment) – W_{OI} (control) (bottom) in a logarithmic time scale; b. the W_{OI} curves from 30 μs to 270 μs; c. fluorescence rise kinetics curves normalized by F_I and F_P (F_M) as W_{IP}; d. the value of δRo).

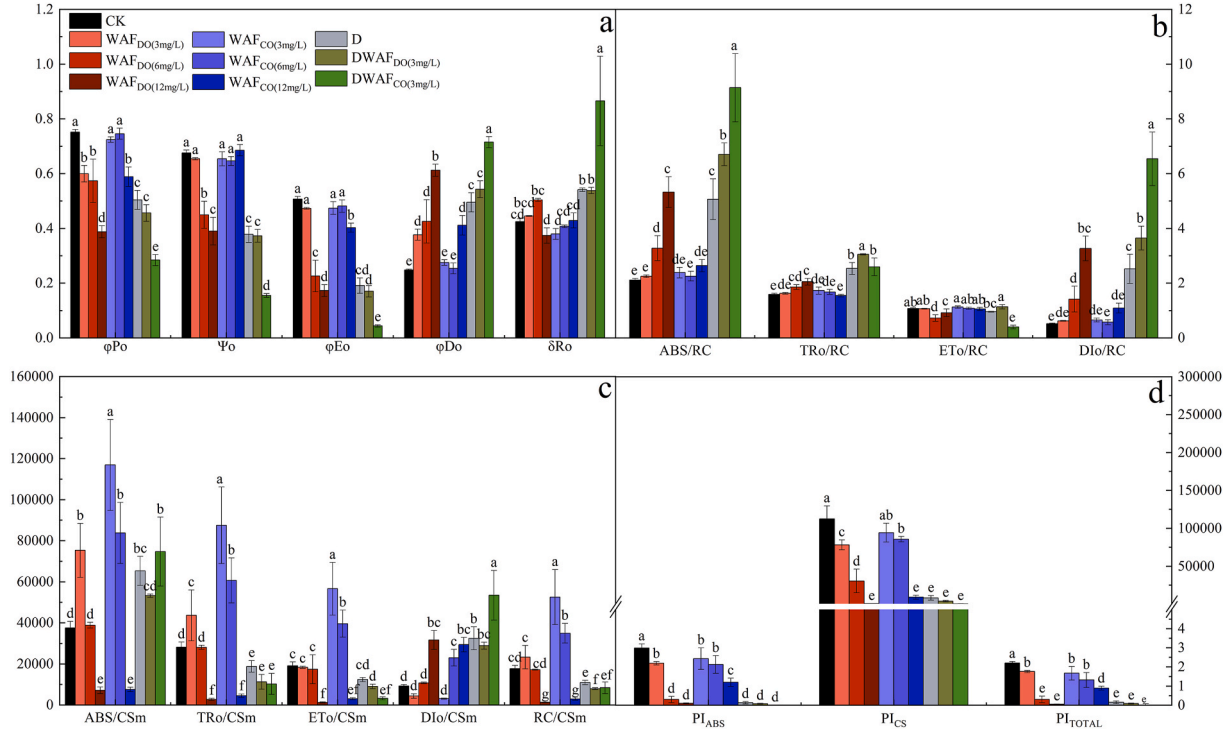

Fig. 9. Effects of petroleum derivatives on the PSII performance indexes of *Ulva prolifera*. (a. quantum yield; b. energy flux per unit reaction centers; c. energy flux per cross-section; d. the performance indexes).

transported (ETo/RC) and dissipated (DIo/RC) flux per RC of *U. prolifera* in response to all petroleum treatments were presented in Fig. 9b. The energy fluxes except ETo/RC had the positive correlation with the WAFs concentration. The values of ABS/RC, TRo/RC and DIo/RC in 6–12 mg/L WAF$_{DO}$, D and DWAFs groups were all significantly higher than control, while the ETo/RC in 6–12 mg/L WAF$_{DO}$ and DWAF$_{CO}$ groups were significantly lower. After the addition of oil-dispersant, the values of ABS/RC, TRo/RC and DIo/RC in the DWAF$_s$ groups greatly increased than the same WAF$_s$ concentration groups, while the value of ETo/RC in DWAF$_{CO}$ greatly decreased than the WAF$_{CO}$ group. Thirdly, the absorbed (ABS/CSm), trapped (TRo/CSm), transported (ETo/CSm), dissipated (DIo/CSm) flux and the number of active reaction centers per cross-section (RC/CSm) of *U. prolifera* were presented in Fig. 9c. The ABS/CSm, TRo/CSm, ETo/CSm and RC/CSm of *U. prolifera* were negatively correlated with the concentration of WAFs, while DIo/CSm showed the positive relationship. In the disperant-addition groups, the values of ABS/CSm, TRo/CSm and RC/CSm in the DWAF$_s$ groups were significantly lower than the same WAF$_s$ concentration groups. While DIo/CSm showed the opposite trend, and the value in the DWAF$_s$ groups were significantly greater than the same WAF$_s$ concentration groups. Finally, three performance indexes based on absorption (PI$_{ABS}$), cross section (PI$_{CS}$) and energy conversion (PI$_{TOTAL}$) are showed in Fig. 9d. The values of three indexes in 3–12 mg/L WAF$_{DO}$, 6–12 mg/L WAF$_{CO}$, D and DWAFs groups were significantly lower than the control group ($P < 0.05$).

3.6. Correlation analysis

The correlation analysis between the physiological and photosynthetic parameters of *U. prolifera* was shown in Fig. 10. In terms of physiological parameters, SGR, pigments and carbohydrate of *U. prolifera* had the strong positive correlation with OEC Centers, φ_{Po}, φ_{Eo} and the comprehensive performance index PI$_{ABS}$, PI$_{CS}$ and PI$_{TOTAL}$, the strong negatively correlation with V_I and φ_{Do}. In addition, SGR, pigments and carbohydrate also had the moderate-strong positive correlation with Ψ_o, ETo/CSm, and moderately strong negative correlation with ABS/RC and DIo/RC. There is a similar pattern in protein, but the correlation was slightly lower. SOD has a strong positive correlation with φ_{Do} and TRo/RC, and a strong negative correlation with OEC Centers, φ_{Po}, φ_{Eo}, PI$_{ABS}$, PI$_{CS}$ and PI$_{TOTAL}$. CAT was not closely related to each photosynthetic parameters, with the absolute value of correlation coefficient less than 0.5.

4. Discussion

The increase of global energy use poses a continuous threat to marine ecosystems. Our research results clearly proved that oil spill-related products have a significant impact on the green tide-causing species *U. prolifera*, especially under the pressure of high concentration of oil and oil-dispersant combinations, its physiological activities and photosynthetic efficiencies are low.

This study first indicated that two oil WAFs have classic dose-response effects on the physiological parameters of *U. prolifera*. The SGR, pigments, carbohydrate and protein contents decreased with the increase of WAF$_s$ concentration, while two antioxidase (SOD and

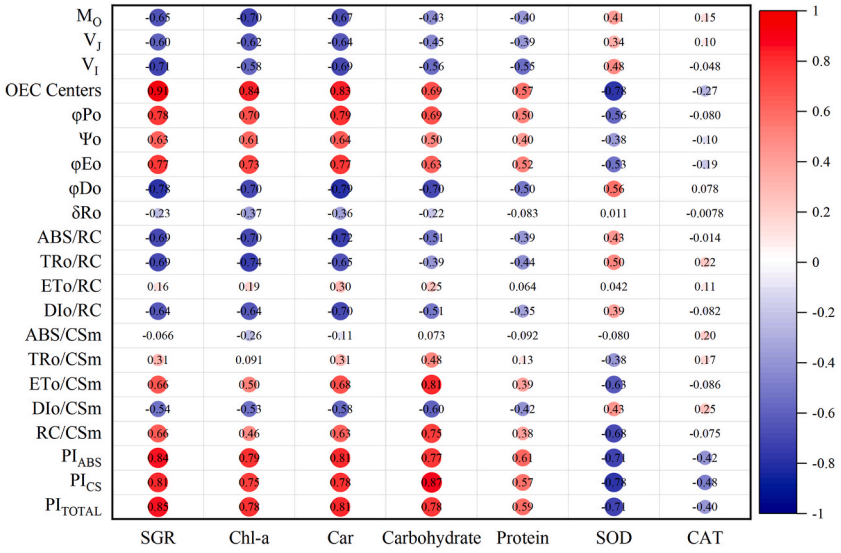

Fig. 10. The correlation analysis between the physiological parameters and photosynthetic performance parameters of *Ulva prolifera*. Data represents the pearson correlation between them.

CAT) activities showed the opposite trends. SGR is the most important index to evaluate the physiological status of macroalgae. The results showed the negative effect of increasing oil stress on the growth of *U. prolifera* was enhanced, which was consistent with the result reported by Liu et al. [14]. At the same time, the change of pigments, carbohydrate and protein content of *U. prolifera* showed the same trends as SGR. Xu and Gao [24] pointed that the damage of carbohydrate and protein was not conducive to the absorption and utilization of light. The reduction of photosynthetic pigments could avoid the over-excitation of electron transfer, thus protecting the photosynthetic mechanism. Moreover, the activities of SOD and CAT increased with WAFs concentration, which was similar to the reports by Luo and Liu [25] and Zheng et al. [26]. The improved SOD activity was to eliminate free radicals rapidly to mitigate damages caused by protein oxidation and carbohydrate damage. Meantime, the increased CAT activity was used for protection against lipid hdyroperosides and hydrogen peroxide [27]. In addition, the addition of dispersant further enhanced the toxicities on *U. prolifera*. Above physiological parameters except two antioxidase activities in the $DWAF_s$ groups were significantly lower than the same concentration WAF_s groups. This result is also consistent with previous reports. Oil disperant GM-2 itself had a negative effective on organism, the addition of GM-2 dispersant enhanced the toxicity of diesel oil and crude oil [28]. Wade et al. [29] reported the dispersion of crude oil and fuel oil resulted in a substantial increase in the total petroleum hydrocarbons and was generally associated with greater physiological impact on algae, compared with the oil alone. The increased toxicity of DWAFs may be mainly due to the high concentration of low molecular hydrocarbons, which poses greater risk to aquatic biota [30].

Through chl-*a* fluorescence parameters have been widely used to investigate the photosynthetic capacity under external stress conditions. However, there are no related reports about oil spill on *Ulva*. This study proved that the stress of petroleum derivatives on photosynthetic performance of *U. prolifera* showed the similar trend with the physiological activity. Two petroleum WAFs also showed significant concentration effects on the chl-*a* fluorescence transients and JIP-test, the mixture of oil and dispersant further increased the stress effects on the photosynthsis. From the aspect of chl-*a* fluorescence transients, first, the decrease in the fluorescence of the OJIP curves indicated that all petroleum derivatives caused photo-oxidation damage of *U. prolifera*. Xia et al. [31] and de Carvalho et al. [32] also pointed the similar phenomenon in *U. prolifera* under salinity and herbicide stress conditions respectively. Secondly, WAF_{DO} at highest concentration and dispersant additive groups blocked the electron transfer beyond QA and from PQ to PSI by increasing the values of V_J and V_I. The interrupted PSII electron transport beyond QA could cause a large accumulation of QA-in PSII RCs, which was consistent with the increased Mo and the destruction of OEC centers. Thirdly, high concentration WAFs and dispersant additive groups increased the L-band and K-band parameters including W_L, ΔW_L and W_K, while changed the IP phase parameters including W_{OI} and W_{IP}. This shows that these stresses reduce the energy transfer efficiency between functional units of PSII, inhibit the pool size and the reduction rate of PSI receptor side, and inactivate the OEC centers on the donor side of PSII [33]. The JIP test parameters subsequently indicate the decrease in photosynthesis may due to the inactivation of PSII reaction centers and the changed energy distribution. First, the quantum yield of *U. prolifera* including φ_{Po}, Ψ_o and φ_{Eo} were significantly inhibited by 12 mg/L WAF_s and dispersant additive groups, while φ_{Do} showed the opposite trend. The similar results was been reported by Xia et al. [31]. Moreover, PI_{ABS}, PI_{CS} and PI_{TOTAL}, as the most sensitive indexes of photosynthesis system, the decreased values mean the functionalities of both PSI and PSII were damaged. In terms of energy flux, petroleum derivatives including highest concentrations WAF_s and dispersant addition groups decreased the number of active reaction centers per CS(RC/CSm), resulting in the decrease of the trapped flux (TRo/CSm) and the transported flux (ETo/CSm). However, the absorbed flux per RC (ABS/RC) and trapped flux (TRo/RC) enhanced at the same time, indicating that *U. prolifera* can ensure the normal supply of light energy by enhancing the function of remaining active response centers under stress. In addition, the active dissipated flux (DIo/RC) observed in *U. prolifera*, by turning excessive light into

thermal energy to increase the light dissipation, which was an adaptive strategy to avoid damaging the photosynthetic structure. This photo-protective mechanism of PSII were also been observed in some *Ulva* species [34]. The change of quantum yield and energy fluxes confirmed that the light energy utilization ability of *U. prolifera* decreased. *U. prolifera* can regulate the inactivation of the reaction center and maintain its energy distribution balance through oil stress.

The correlation analysis revealed several photosynthetic parameters were closely related to physiological parameters. Among them, φ_{Po} of algae is a relatively stable value under non-stress conditions, and will decrease under stress conditions; so, it is often used as a stress indicator [25,35]. In this study, the φ_{Po} of *U. prolifera* was sharply decreased in WAFs, D and DWAFs groups, indicating that those treatments caused significant stress to *U. prolifera*. Especially in DWAFs groups, not only the lower growth rate was found, but also the lowest pigments, protein and carbohydrate contents were obtained. These results undoubtedly showed that the oil stress caused both photosynthetic and physiological damage. Besides φ_{Po}, the comprehensive performance index PI_{ABS}, PI_{CS} and PI_{TOTAL} are also considered to be indicators of stress conditions, even more sensitive than φ_{Po}. In this study, three indexes values in high concentration WAFs and dispersant addition groups were lower than the control group, which also proved the stress nature of oil spill-related products for *U. prolifera* to grow and accumulate cell contents. Furthermore, OEC centers and φ_{Eo} are connected to the process of electron transport, which also closely related to growth and nutritional accumulation. In addition, among other photosynthetic parameters closely related to physiological status, ABS/RC is the energy absorbed per reaction centers, and parameters of φ_{Do}, DIo/RC and DIo/CSm are all related to energy dissipation. This also suggests that growth, pigment and carbohydrate accumulation are mainly related to the balance between energy absorption and dissipation in the photosynthetic system.

Although inhibition is the main effect caused by petroleum derivatives, stimulation at low WAF concentration is also common [36]. Our results also showed this phenomenon. Among our WAF_{CO} treated groups, 3 mg/L crude oil stimulate the growth, pigments, carbohydrate and protein contents of *U. prolifera*, while 6–12 mg/L crude oil reduce these parameters. This "toxicant excitatory effect" was been confirmed in microalgae and observed in some *Ulva* species [22,37]. The reason for the growth of algae is that petroleum hydrocarbons can affect the synthesis of proteins, carbohydrate, and other biological macromolecules, and the synthesis rate directly reflects the metabolism and growth of the algae. Pilatti et al. [38] found carbohydrates metabolism as the main detoxification pathway in *U. lactuca*. de Carvalhov et al. [32] suggest that *U. lactuca* is able to metabolize hydrocarbons and use them as energy source, acting as bio-remediator of marine waters contaminated by petroleum derivatives. Lv et al. [28] reported that algae accelerate the accumulation of proteins in their bodies to promote their ability to detoxify petroleum stress. This "toxicant excitatory effect" stimulate the growth of *U. prolifera*, making it more likely to induce the formation of green tide.

The above results emphasized that oil spill, especially crude oil at lower concentrations, makes it more likely to induce the formation of green tide. However, the addition of dispersant would greatly reduce the physiological characteristics of *U. prolifera*. Therefore, from the perspective of oil spill clean-up strategy, a coastal crude oil spill accident may lead to the formation of *U. prolifera* green tide, but the oil dispersant GM-2 used after the oil spill is unlikely to further stimulate the bloom scale. **5 Conclusion**.

Our study investigated the comparative toxic effects of diesel oil, crude oil, dispersant, and combinations of oil-dispersant on the physiology and photosynthetic characteristics of *U. prolifera*. This method of contaminant addition was employed to simulate the impact of oil spills in the natural environment. The toxicity tests revealed the following results: 1) Crude oil exhibited low concentration induction and high concentration inhibition effects on physiological parameters, including growth rate and cell contents, while the presence of dispersant decreased these physiological activities. This finding suggests that crude oil spills may trigger the occurrence of *U. prolifera* green tides, and the application of oil dispersant following such spills is unlikely to further enhance the scale of the bloom. 2) Diesel oil consistently exhibited a negative concentration effect on the physiological characteristics and photosynthetic efficiency of *U. prolifera*, with dispersant further inhibiting these activities. This outcome indicates that diesel oil spills may not promote the formation of *U. prolifera* green tides in the Yellow Sea.

5. Limitations and future works

In addition to the above findings, the study has potential limitations. An apparent limitation of the method is using simulated medium instead a real seawater. Consequently, this study is confined to a microscopic toxicity test in the laboratory, rather than reflecting the real ecological environment under natural conditions. Furthermore, we only studied the toxic effects of two oils and did not measure the changes of oil component and concentration in this experiment, for which further study are needed. Eventually, the "toxicant excitatory effect" and stress mechanism triggered by oil spills were not be identified from recent results. Therefore, more experimental elucidations are needed by using some advanced methods such as transcriptomic or metabolome analysis in the next works.

Data availability statement

The data used and analyzed in the current study will be made available on request.

CRediT authorship contribution statement

Qing Liu: Writing – original draft, Conceptualization, Data curation, Formal analysis, Investigation, Methodology, Validation. **Ruifei Cui:** Writing – original draft, Methodology, Investigation, Conceptualization, Data curation, Formal analysis. **Yuxin Du:** Investigation, Data curation, Formal analysis, Validation. **Junjie Shen:** Investigation, Data curation, Formal analysis, Methodology. **Cuili Jin:** Conceptualization, Data curation, Formal analysis, Investigation, Methodology, Funding acquisition. **Xiaojian Zhou:**

Writing – review & editing, Conceptualization, Data curation, Methodology, Validation, Writing – original draft.

Declaration of competing interest

The authors declare that they have no known competing financial interests or personal relationships that could have appeared to influence the work reported in this paper.

Acknowledgements

We thank associate professor Cathy Wu for language modification. The study was supported by the National Natural Science Foundation of China (No. 42177459).

References

[1] B. Zhao, Qingdao pipeline explosion: introductions and reflections, Nat. Hazards 74 (2) (2014) 1299–1305.
[2] W. Gao, X.F. Yin, T.Z. Mi, Y.R. Zhang, F.X. Lin, B. Han, X.L. Zhao, X. Luan, Z.S. Cui, L. Zheng, Microbial diversity and ecotoxicity of sediments 3 years after the Jiaozhou Bay oil spill, Amb. Express 8 (1) (2018) 1–10.
[3] Z.K. Liu, Q. Chen, Y.W. Zhang, C. Zheng, B.P. Cai, Y.H. Liu, Research on transport and weathering of oil spills in Jiaozhou Bight, China, Reg. Stud. Mar. Sci. 51 (2022) 102197.
[4] Z.W. Zhu, F. Merlin, M. Yang, K. Lee, B. Chen, B. Liu, Y.Q. Cao, X. Song, X.D. Ye, Q.Q. Li, C.W. Greer, M.C. Boufadel, L. Isaacman, B.Y. Zhang, Recent advances in chemical and biological degradation of spilled oil: a review of dispersants application in the marine environment, J. Hazard Mater. 436 (2022) 129260.
[5] D.M. Anderson, E. Fensin, C.J. Gobler, A.E. Hoeglund, K.A. Hubbard, D.M. Kulis, J.H. Landsberg, K.A. Lefebvre, P. Provoost, M.L. Richlen, J.L. Smith, A. R. Solow, V.L. Trainer, Marine harmful algal blooms (HABs) in the United States: history, current status and future trends, Harmful Algae 102 (2021) 101975.
[6] C. Suzuki, Assessing change of environmental dynamics by legislation in Japan, using red tide occurrence in Ise Bay as an indicator, Mar. Pollut. Bull. 102 (2) (2016) 283–288.
[7] X. Liu, C.C. Zhang, R.Y. Geng, X. Lv, Are oil spills enhancing outbreaks of red tides in the Chinese coastal waters from 1973 to 2017? Environ. Sci. Pollut. R. 28 (40) (2021) 56473–56479.
[8] W.M. Graham, R.H. Condon, R.H. Carmichael, I. D'Ambra, H.K. Patterson, L.J. Linn, F.J. Hernandez, Oil carbon entered the coastal planktonic food web during the Deepwater Horizon oil spill, Environ. Res. Lett. 5 (4) (2010) 045301.
[9] L. Zhou, D.L. Tang, J. Sun, Investigation of marine phytoplankton blooms after the oil spills in the seas, Ecol. Sci. 32 (6) (2013) 692–702.
[10] B.S. Park, D.L. Erdner, H.P. Bacosa, Z. Liu, E.J. Buskey, Potential effects of bacterial com-munities on the formation of blooms of the harmful dinoflagellate *Prorocentrum* after the 2014 Texas City "Y" oil spill (USA), Harmful Algae 95 (2020) 101802.
[11] X.Y. Li, R.C. Yu, H.X. Geng, Y.F. Li, Increasing dominance of dinoflagellate red tides in the coastal waters of Yellow Sea, China, Mar. Pollut. Bull. 168 (2021) 112439.
[12] Y.Q. Zeng, Z.H. Chen, J.X. Cao, S. Li, Z.Y. Xia, Y.Q. Sun, J.H. Zhang, P.M. He, Revolutionizing early-stage green tide monitoring: eDNA metabarcoding insights into *Ulva prolifera* and microecology in the South Yellow Sea, Sci. Total. Enviro. 912 (2024) 169022.
[13] L.X. Zheng, M.Q. Wu, Y.T. Cui, L. Tian, P.S. Yang, L.J. Zhao, M.Y. Xue, J.Y. Liu, What causes the great green tide disaster in the South Yellow Sea of China in 2021, Eco. Ind 140 (2022) 108988.
[14] Y.X. Liu, Y. Liu, N. Li, Y.D. Lou, X.D. Zhao, Effect of oil spill stress on fatty acid stable carbon isotope composition of *Ulva pertusa*, Sci. Total Environ. 649 (2019) 1443–1451.
[15] R.R.L. Guillard, Culture of phytoplankton for feeding marine invertebrates, in: W.L. Smith, M.H. Chanley (Eds.), Culture of Marine Invertebrate Animals, Plenum Press, New York, NY, 1975, pp. 26–60.
[16] M.M. Singer, D. Aurand, G.E. Bragin, J.R. Clark, G.M. Coelho, M.L. Sowby, R.S. Tjeerdema, Standardization of the preparation and quantitation of water-accommodated fractions of petroleum for toxicity testing, Mar. Pollut. Bull. 40 (11) (2000) 1007–1016.
[17] K.G. Wilson, P.J. Ralph, Laboratory testing protocol for the impact of dispersed petrochemicals on seagrass, Mar. Pollu. Bull 64 (11) (2012) 2421–2427.
[18] R.J. Porra, The chequered history of the development and use of simultaneous equations for the accurate determination of chlorophylls a and b, Photosynth. Res. 73 (1–3) (2002) 149–156.
[19] T.R. Parsons, J.D.H. Strickland, Discussion of spectrophotometric determination of marine-plant pigments, with revised equations far ascertaining chlorophylls and carotenoids, J. Mar. Res. 21 (3) (1963) 155–163.
[20] M. DuBois, K.A. Gilles, J.K. Hamilton, P.A. Rebers, F. Smith, Colorimetric method for deter-mination of sugars and related substances, Anal. Chem. 28 (3) (1956) 350–356.
[21] M.M. Bradford, A rapid and sensitive method for the quantitation of microgram quantities of protein utilizing the principle of protein-dye binding, Anal. Biochem. 72 (1–2) (1976) 248–254.
[22] K. Ramadass, M. Megharaj, K. Venkateswarlu, R. Naidu, Sensitivity and antioxidant response of *Chlorella* sp. MM3 to used engine oil and its water accommodated fraction, Bull. Environ. Contam. Toxicol. 97 (1) (2016) 71–77.
[23] A. Stirbet, On the relation between the Kautsky effect (chlorophyll a fluorescence induction) and photosystem II: basics and applications of the OJIP fluorescence transient, J. Photochem. Photobiol. B Biol. 104 (1–2) (2011) 236–257.
[24] J.T. Xu, K.S. Gao, Future CO_2-induced ocean acidification mediates the physiological performance of a green tide alga, Plant. Physiol. 160 (4) (2012) 1762–1769.
[25] M.B. Luo, F. Liu, Salinity-induced oxidative stress and regulation of antioxidant defense system in the marine macroalga *Ulva prolifera*, J. Exp. Mar. Biol. Ecol. 409 (1–2) (2011) 223–228.
[26] M.S. Zheng, J.J. Lin, S.D. Zhou, J.L. Zhong, Y.H. Li, N.J. Xu, Salinity mediates the effects of nitrogen enrichment on the growth, photosynthesis, and biochemical composition of *Ulva prolifera*, Environ. Sci. Pollut. R. 26 (2019) 19982–19990.
[27] H.T. Xu, L.A. Li, Y.J. Wang, K.C. Qiu, S.Y. Chen, J.N. Zeng, R.J. Liu, Q.K. Yang, W. Huang, Differential physiological response of marine and freshwater microalgae to polystyrene microplastics, J. Hazard Mater. 448 (2023) 130814.
[28] X. Lv, X. Liu, X.K. Hu, R.Y. Geng, C. Tang, Q.G. Xing, The red tide organism *Chaetoceros* sp. responding to exposure to oil and dispersant, Sustainability 15 (2) (2023) 1103.
[29] T.L. Wade, S.K. Driscoll, J. McGrath, T. Coolbaugh, Z. Liu, E.J. Buskey, Exposure methodologies for dissolved individual hydrocarbons, dissolved oil, water oil dispersions, water accommodated fraction and chemically enhanced water accommodated fraction of fresh and weathered oil, Mar. Pollut. Bull. 184 (2022) 114085.
[30] C.M. Couillard, K. Lee, B. Légaré, T.L. King, Effect of dispersant on the composition of the water-accommodated fraction of crude oil and its toxicity to larval marine fish, Environ. Toxicol. Chem. 24 (6) (2005) 1496–1504.
[31] J.R. Xia, Y. Li, D.H. Zou, Effects of salinity stress on PSII in *Ulva lactuca* as probed by chlorophyll fluorescence measurements, Aquat. Bot. 80 (2) (2004) 129–137.
[32] R. Cruz de Carvalho, E. Feijão, A.R. Matos, M.T. Cabrita, A.B. Utkin, S.C. Novais, M.F.F. Lemos, I. Cacador, J.C. Marques, P. Reis-Santos, V.F. Fonseca, B. Duarte, Effects of glyphosate-based herbicide on primary production and physiological fitness of the macroalgae *Ulva lactuca*, Toxics 10 (8) (2022) 430.

[33] Y.J. Guo, Y.P. Lu, V. Goltsev, R.J. Strasser, H.M. Kalaji, H. Wang, X.X. Wang, S.G. Chen, S. Qiang, Comparative effect of tenuazonic acid, diuron, bentazone, dibromothymoquinone and methyl viologen on the kinetics of Chl *a* fluorescence rise OJIP and the MR820 signal, Plant. Physiol. Bioch. 156 (2020) 39–48.
[34] Z.H. Zhong, L. Sun, Z.Y. Liu, Z.M. Song, M.Y. Liu, S.Y. Tong, S. Qin, Ocean acidification exacerbates the inhibition of fluctuating light on the productivity of *Ulva prolifera*, Mar. Pollut. Bull. 175 (2022) 113367.
[35] S. Gao, Z.B. Zheng, W.H. Gu, X.J. Xie, L. Huan, G.H. Pan, G.C. Wang, Photosystem I shows a higher tolerance to sorbitol-induced osmotic stress than photosystem II in the intertidal macro-algae *Ulva prolifera* (Chlorophyta), Physiol. Plantarum 152 (2) (2014) 380–388.
[36] M.M. El-Sheekh, A.H. El-Naggar, M.E. Osman, A. Haieder, Comparative studies on the green algae *Chlorella homosphaera* and *Chlorella vulgaris* with respect to oil pollution in the river Nile. Water. Air, Soil Poll. 124 (2000) 187–204.
[37] Z.B. Jiang, Y.J. Huang, X.Q. Xu, Y.B. Liao, L. Shou, J.J. Liu, Q.Z. Chen, J.N. Zeng, Advance in the toxic effects of petroleum water accommodated fraction on marine plankton, Acta Ecol. Sin. 30 (1) (2009) 8–15.
[38] F.K. Pilatti, F. Ramlov, E.C. Schmidt, M. Kreusch, D.T. Pereira, C. Costa, E.R. Oliveira, C.M. Bauer, M. Rocha, Z.L. Bouzon, M. Maraschin, In vitro exposure of *Ulva lactuca* Linnaeus (Chlorophyta) to gasoline–Biochemical and morphological alterations, Chemosphere 156 (2016) 428–437.